Prototype Development of a Thermoluminescence Dosimeter Based on Monte Carlo Simulation Methods

C. Hranitzky[1], H. Stadtmann[1], P. Kindl[2]

[1]Health Physics Division, ARC Seibersdorf research GmbH, 2444 Seibersdorf, Austria
E-mail: christian.hranitzky@arcs.ac.at
[2]Institute of Technical Physics, Graz University of Technology, Petersgasse 16, 8010 Graz, Austria

Abstract. The European Directive 96/29/EURATOM and adapted national regulations on radiation protection are claiming new limits of radiation exposure and the introduction of new measuring quantities. Dosimeters for area monitoring of penetrating X-ray and gamma radiation have to measure the ICRU operational quantity ambient dose equivalent, *H*(10)*. In this paper, the development stages of a passive *H*(10)* area dosimeter based on thermoluminescence detectors (TLDs) are described. The design of the dosimeter and the optimization of the combined energy and directional response are almost completely performed by MCNP Monte Carlo computer simulations. At the end of the first prototype development stage, two prototypes containing three TLD cards were manufactured according to the simulation results. The optimization method and dosemeter properties could be confirmed by the concluding verification experiment. The prototypes of the second development phase were especially optimized for measuring independent of the direction of incident photon radiation fields. Additionally, an aluminium cap was introduced for environmental protective purposes. The third-stage prototypes currently under testing were planned as the final stage of the presented dosimeter development process. Their design was optimized on meeting specific requirements of passive area monitoring devices in routine applications.

1. Introduction

The aim of this work was the development of a new passive radiation protection dosimeter for area monitoring using thermoluminescence detectors. Three prototype stages are described here together with the dosemeter optimization method based on Monte Carlo simulations. Instead of time-consuming experiments, dosemeter materials, geometries, and detector positioning were varied and optimized by close to reality computer simulations. The main goals of the three dosemeter prototype stages were the optimization of the photon energy response, the optimization of the directional response, and the optimization of the handling and usability as routine area dosemeters.

The European Council Directive 96/29/EURATOM [1] and adapted national regulations are laying down new safety standards for radiation protection. New dose limits of radiation exposure from artificial radiation sources are introduced as well, e.g. the limit on effective dose for members of the public is set to 1 mSv per year. For the estimation of the non-measurable effective dose, the operational quantities for external radiation are internationally recommended, e.g. the ambient dose equivalent *H*(10)* for area monitoring of strongly penetrating radiation fields.

Passive thermoluminescence dosemeters (TLDs) are in many cases the best choice for area monitoring applications, mainly because they are small, robust, and relatively cheap. Between annealing and readout the thermoluminescence (TL) detectors accumulates dose. At the end of the measuring period, i.e. between one month and one year, the TL signals can be evaluated as a measure of absorbed dose. Long-term dose integration is a well suited method, because of the generally occurring low dose rate values in the range of the natural radiation background, i.e. about 1.5 µSv/d. In contrast to active systems, there is no online information of the current dose rate available.

An overview over current active and passive ambient monitoring devices was given in the publication of Saez-Vergara [2]. Topical publications concerning different *H*(10)* dosemeter types and their dosimetric properties were reviewed by Hranitzky [3]. Especially the 2 cm diameter PMMA mini-phantom of Carlsson *et al.* [4] and the *H*(10)* ionisation chamber of Duftschmid *et al.* [5] stimulated the first developments of TLD based *H*(10)* prototypes described in this work.

2. Area monitoring

In the field of radiation protection, area monitoring (environmental and workplace monitoring) of radiation exposure due to external radiation fields is carried out by means of area dosemeters. The occupational exposure of people working in radiation areas is individually monitored by means of personal dosimeters, which have to be worn on the body during working hours. On the other hand, area dosemeters are placed at fixed locations controlling the possible exposure of persons staying at those locations. Therefore, the use of area dosemeters allows the controlling of the compliance with legally radiation protection limits not only for radiation workers, but also for classified radiation areas and for members of the general public.

Area monitoring dosemeters are currently applied mainly in and around nuclear plants, high energy accelerator facilities and close to medical radiation sources. They are more and more employed in addition to or as substitute for individual dosemeters as a measure of guarantee for radiation protection responsible persons.

2.1. Radiation Background Influences

A general problem of low dose evaluations in area and personal dosimetry is the presence of the natural background exposure, which is overlaying the interesting occupational radiation exposure. However in area monitoring dosimetry, reference measurements for estimating the local background exposures can be carried out in many cases before authorization and initial operation or during power-off periods.

A simple background correction model as proposed by the German DIN 25483 standard [6], i.e. subtraction of an average background dose value from the measured dose value, introduces additional uncertainties. In Austria, measured dose values are generally reported including the natural background component integrated over the measuring period, i.e. normally one month for personal dosemeters and three months for area dosemeters. Stadtmann *et al.* [7] identified natural and occupational exposure related components in statistically evaluated dose distributions of different occupational groups.

3. The measuring quantity *H*(10)*

The operational quantity ambient dose equivalent *H*(10)* was introduced by the International Commission on Radiation Units and Measurements (ICRU) as an appropriate estimate of the protection quantity effective dose for penetrating ionizing radiation, such as photons of energies above 15 keV. For photon energies below some MeV and for all whole body irradiation conditions, the ambient dose equivalent is a conservative estimate, i.e. *H*(10)* values are always slightly higher than corresponding effective dose values. The ICRU [8] defined *H*(10)* as dose equivalent (*H*(10) = Q·D)* in a point of a radiation field by means of the 30 cm diameter ICRU-tissue sphere phantom. The absorbed dose *D* at 10 mm depth in the ICRU sphere is weighted by the mean radiation quality factor *Q* of the incident radiation. For photons *Q* is set equal to 1.

According to a number of international publications in the field of environmental monitoring of external radiation fields, the ambient dose equivalent *H*(10)* will replace field quantities such as the air kerma free-air K_a for photon radiation fields. Even the new American ANSI N.13.29 standard [9] for environmental dosimetry introduces *H*(10)* as preferable measuring quantity.

3.1. H(10) conversion coefficients*

H(10)* conversion coefficients $h^*_K(10)$ allow the determination of the ambient dose equivalent *H*(10)* at a point in a radiation field, if the following information is available: particle type of radiation, e.g. photons, energy distribution or mean energy *E* of the particles at the specified point, and field strength at the specified point, e.g. the air kerma free-in-air value K_a.

$$h^*_K(10,E) = \frac{H^*(10,E)}{K_a(E)} \quad (1)$$

Due to its definition, *H*(10)* is independent of the direction of the incident radiation. Tables of energy dependent conversion coefficients $h^*_K(10,E)$ from air kerma free-in-air to ambient dose equivalent were given by the ICRU [8] and the ISO 4037-3 standard [10]. Those data were calculated by Monte Carlo simulations based on the strict definition of *H*(10)* by the ICRU-sphere phantom. Compared to air kerma free-in-air, *H*(10)* shows an under-response at low photon energies, i.e. below 30 keV, due to increased radiation absorption before reaching the measuring point at 10 mm depth in tissue. At higher photon energies, radiation scattering from the tissue phantom creates an over-response with a maximum of about 70 % at photon energies around 60 keV.

3.2. H(10) dosemeter requirements*

The aim of the work was to design an *H*(10)* area dosemeter, which is applicable for unknown photon radiation fields. This means, the final dosimeter shall measure the ambient dose equivalent at the measuring location in principle independently of the incident radiation energy E and independently of the direction of radiation incidence α. The prototype stages of this work present the optimizations of the relative combined *H*(10)* energy and directional response $R(E,\alpha)$ of the detector signal $TL(E,\alpha)$. Values close to the ideal value $R = 1$ shall be achieved for all irradiation conditions. The reference values for *H*(10)* were taken from the ISO [10] conversion coefficients $h^*_K(10,E)$, see equation (1).

$$R(E,\alpha) = \frac{TL(E,\alpha)/H^*(10,E)}{TL(Cs,0°)/H^*(10,Cs)} = \frac{TL(E,\alpha)/K_a(E)}{TL(Cs,0°)/K_a(Cs)} \cdot \frac{h^*_K(10,Cs)}{h^*_K(10,E)} \quad (2)$$

The properties of routine area dosemeters are described in standards such as the ÖNORM S 5237-2 standard [11] and the DIN 25483 standard [6]. There, minimum requirements for measuring ranges, reference conditions, dose linearity, variation coefficients for repeated measurements, and other properties are fixed. For energy and angular variations a maximum deviation of 40% from the reference energy of the radionuclide ^{137}Cs gamma radiation (E = 662 keV) and the reference direction of the dosemeter (defined as $\alpha = 0°$) is allowed, i.e. $0.6 \leq R(E,\alpha) \leq 1.4$.

4. Thermoluminescence dosimetry

Thermoluminescence dosemeters (TLDs) generally consist of one or more single TL detectors placed inside the dosemeter. The emitted TL light intensities of the detectors are measured during heating after dosemeter irradiations. In this work, a Harshaw 8800 automatic hot gas reader for Harshaw TLD cards were used. The time-temperature readout profile for the TLD cards consisted of a preheat plateau at 165°C, a heating rate of 5°C/s, and a maximum gas temperature of about 275°C. The readout parameters were optimized for simultaneous use of the two TL detector materials LiF:Mg,Ti (Harshaw, TLD-100) and LiF:Mg,Cu,P (Harshaw, TLD-100H). The TL signals were evaluated by summing up the TL intensities around the main peak of the TL glow curve, described in detail by Hranitzky [3].

Air kerma free-in-air calibration values $K_a(E)$ of about 1 mGy to 2 mGy at the centre of the irradiated dosemeters were used in all experiments and applied to *H*(10)* response calculations according equation (2). In addition, constant time intervals of 1 day between annealing and irradiation and between irradiation and readout were applied. Therefore, TL related influences, e.g. fading and dose non-linearity, could be neglected for the prototype development, but will be investigated in the future for the final version of the area dosemeter.

4.1. TL efficiency

The TL efficiency η is quantifying the ability of an irradiated material to produce a TL light signal after thermal stimulation. Differences between the absorbed dose D and the measured TL light output

are due to complex processes involved in storing absorbed radiation energies at so-called TL centres in the crystal structure and in releasing stored energies by thermal excitation processes.

$$\frac{TL(E)}{TL(Cs)} = \eta(E) \cdot \frac{D(E)}{D(Cs)} \tag{3}$$

The photon energy dependence of the relative TL efficiency $\eta(E)$ can only be determined directly for ideal photon irradiation geometries and by using monoenergetic photons of energies E. For making Monte Carlo simulations available as a tool for calculating the $H^*(10)$ response of a TLD based dosemeter, a new method was developed by Hranitzky *et al.* [12] for determining photon TL efficiencies for LiF:Mg,Ti and LiF:Mg,Cu,P.

5. Monte Carlo simulation technique

Monte Carlo simulation codes are nowadays widely used as reliable and accurate computational tools in radiation dosimetry. The general purpose Monte Carlo transport code MCNP [13] was used to calculate spectral absorbed dose distributions in the TL detector volumes. Previously determined photon TL efficiencies allowed the implementation of a new computer simulation based optimization method [12] instead of time-consuming experiments.

MCNP calculates the primary and secondary photon transport (and optionally the electron and neutron transport) through the materials of the dosimeter and surrounding geometries above the pre-selected cut-off transport energy of 1 keV. For all experimental and close to reality simulated irradiations, ISO 4037-1 standard [14], [15] narrow x-ray spectra N-30 to N-300 and radionuclide radiation qualities S-Cs and S-Co with mean photon energies between 24 keV and 1.25 MeV were applied.

Extensive Monte Carlo simulations were carried out to optimize the dosemeter energy and directional response by varying free dosemeter parameters, e.g. materials, shapes, dimensions and TL detector positioning. Some time optimization techniques were introduced to achieve relative statistical uncertainties below 1%.

5.1. Simple simulation models

A series of attenuation and backscatter studies were necessary for finding suitable dosimeter and filter materials. Spherical and cylindrical dosimeter shapes were chosen for the first simple simulation models because of their high symmetry for achieving low directional dependences. Single TL detector volumes were placed at the dosemeter centre; multiple TL detectors were isotropically distributed in the dosemeter volume. Summing over all detector volumes was the applied principle for getting directional independent dose signal. A compilation of the simulated energy dependences of the simple dosemeter models (e.g. an optimized spherical H*(10) dosemeter consisting of a central LiF detector, a 15 μm tin metal layer, and 5 mm PMMA filter layer) can be found in Hranitzky *et al.* [16]. The influence of the TL efficiency was not taken into account at that early stage of development.

6. Prototype development stages

6.1. Current H_x area dosemeter

The current H_x area dosemeter of the dosimetry service of Seibersdorf was introduced many years ago. Seibersdorf was the first European dosimetry service using TLDs for routine personal dosimetry, i.e. for more than 30 years now. The dosemeter response is calibrated in terms of the currently legal quantity photon dose equivalent H_x. Due to its direct relationship to the quantity exposure, H_x can be related to the air kerma free-in-air for radiation protection relevant photon energies by $H_x = 1.14 \cdot K_a$.

Figure 1 shows the components of the currently used H_x area dosemeter. The dosemeter contains five aluminium TLD cards each holding four LiF:Mg,Ti (Harshaw, TLD-100) chips. After the readout annealing process, all TLD cards get packed into Mylar-aluminium foils protecting the TL detector elements from dust, dirt, water, and light. During the packing procedure, the measuring location, the measuring period, and other useful information are printed on the packing foil. The readout procedure in the automatic 8800 Harshaw hot gas readers is similar to the one used for routine personal dosemeters.

FIG. 1. Photograph of the Seibersdorf H_x area dosemeter. From left to right: aluminium case, PMMA holder for five TLD cards, a packed TLD card, and an unpacked TLD card.

The five TLD cards are symmetrically arranged inside the cylindrical PMMA holder. An aluminium casing is fixed on the PMMA holder protecting the detectors from light, heat, rain-water, snow, and other mechanical and environmental influences. Two of the five TLD cards, i.e. eight of the twenty TL detector elements, are pre-irradiated with H_x = 5 mSv. Because these two calibration cards are exposed to the same temperature and humidity conditions as the three measuring cards, their TL signals can be used for fading correction. The final dose value is the average over all TL detector element signals of the measuring cards after applying several corrections.

A drawback of the current H_x area dosemeter is the not optimized angular dependence for non-isotropic radiation fields. For very extreme cases of incident radiation fields, i.e. from the bottom (ground) or the top (air), some deviations in the measured dose values may be expected. For generally using the quantity H_x as an estimate of the effective dose, deviations greater than 80% have to be taken into account.

6.2. Stage-1 prototypes

The cylindrical shape for the stage-1 prototypes was chosen because of its high (rotational) symmetry on the one hand and the easy and cheap production on the other hand. Similar to the currently used H_x area dosemeter for routine purposes, TLD cards should be employed from the beginning of the prototyping instead of single TL detector chips. The fixed positions and orientations of the four TL detector chips mounted between Teflon foils in the flat aluminium holder (Harshaw) introduced additional difficulties in the optimization of an isotropic *H*(10)* dosemeter response.

The TL detector material LiF:Mg,Ti (TLD-100) was preferred from the beginning of the prototype development, because of its advantageous energy dependence, i.e. an increasing over-response compared to air kerma free-air for decreasing photon energies. Free-in-air measurements of the new high-sensitive TL detector material LiF:Mg,Cu,P (TLD-100H) confirmed the anomalous energy response with an under-responses of 20% at 100 keV photon energies. More complicated dosemeter designs would be necessary to employ this detector material for *H*(10)* dosemeters. Future prototypes may be developed based on this promising material because of its about 20 times higher photon detection sensitivity making measuring periods of a few days possible.

At the end of the stage-1 prototype development phase, two prototypes were manufactured completely based on Monte Carlo simulation results. Figure 2 shows the prototype version made of polymethyl methacrylate (PMMA). These first prototypes were made of three parts: the inner cylindrical part containing three slits for precise positioning of the TLD cards, the outer hollow cylindrical part, and a cylindrical cover for closing the dosemeter.

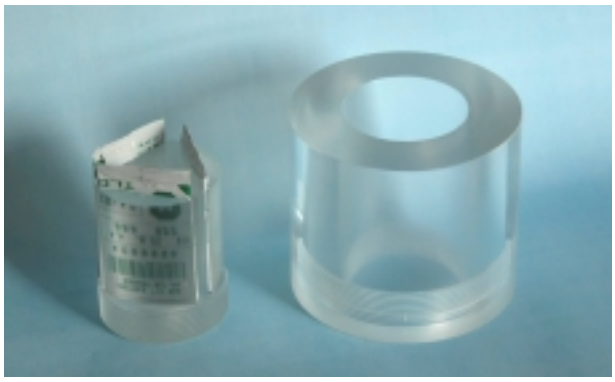

FIG. 2. Photograph of the stage-1 prototype area dosemeter made of PMMA. Left: Inner cylindrical part containing three packed TLD cards. Right: Outer cylindrical part.

The modularity of the construction was chosen for eventually adapting the dimensions of the outer cylindrical part of the dosemeter keeping the more complicated inner part unchanged. The 43.5 mm diameter of the inner dosemeter parts were optimized for holding three TL cards, which were arranged as an equilateral triangle.

A number of Monte Carlo simulations were carried out for testing various detector positioning concepts (rectangular, triangular, star shaped) and number of TL cards (one to six) inside the dosemeter, see Hranitzky [3]. The outer diameter and height were optimized by Monte Carlo simulations for two different materials: PMMA and polyethylene (PE). Other appropriate but less applicable dosemeter materials were tested by simulation comparisons, e.g. graphite and PVC.

The dimensions were varied for the whole photon energy range and for the four defined main angles 0°, 30° *horiz*, 60° *horiz*, and 90° *vert*. *horiz* is the short name for incident angles in the horizontal plane, i.e. perpendicular to the rotational axis. *Vert* angles are lying in the vertical plane defined by the rotational axis and the dosemeter reference direction 0°. The best dosemeter response values *R* were found for the following dimensions: 80 mm diameter and 70 mm height for PMMA, 130 mm diameter and 110 mm height for PE. Minimum (R_{min}) and maximum (R_{max}) response values for the applied photon radiation qualities and for the main angles were presented in table I.

Table I. Range of simulated H(10) dosemeter response values R_{min} to R_{max} for mean photon energies between 33 keV and 1.25 MeV optimized for 4 angles of radiation incidence and 2 dosemeter materials.*

	0°		**30° *horiz***		**60° *horiz***		**90° *vert***	
	R_{min}	R_{max}	R_{min}	R_{max}	R_{min}	R_{max}	R_{min}	R_{max}
PMMA	0,88	1,03	0,86	1,02	0,88	1,03	0,77	1,04
PE	0,92	1,12	0,92	1,09	0,92	1,12	0,96	1,11

The extreme angle of radiation incidence 90° *vert* seemed to be problematic for the PMMA dosemeter, but not for the bigger PE dosemeter. However, for this singular extreme angle, clear differences between idealized simulation and experimental values were expected. Tests for 75°*vert* showed good response values especially for low energies (R_{min} = 0.89) for the PMMA dosemeter but higher deviations (R_{max} = 1.15) for the PE dosemeter. At the end of the simulation optimization process the

verification experiment was carried out. Energy dependences for the dosemeter reference direction and some interesting angles were measured. Figure 3 shows the simulated and measured energy response values for 0° for the two stage-1 prototypes.

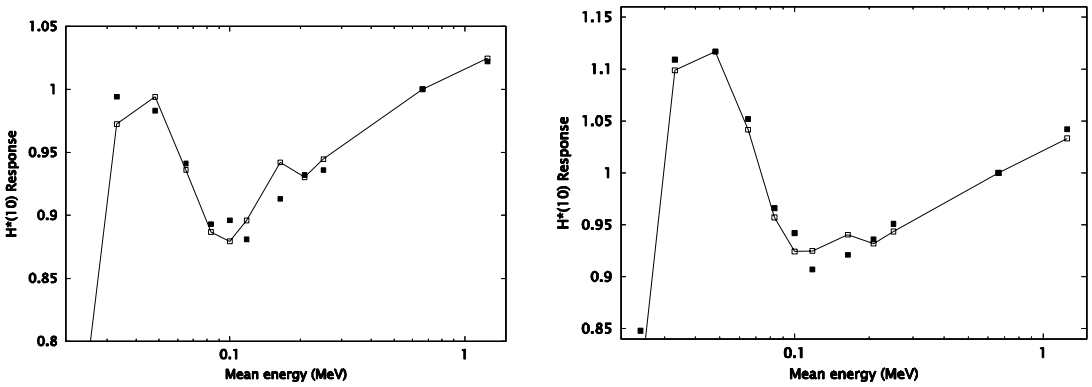

FIG. 3. Measured (full symbols) and simulated (open symbols) energy dependence of the H(10) dosemeter response R(E,0°) for the PMMA (left figure) and PE (right figure) stage-1 prototype.*

The mean value of the absolute differences between simulated response values and verification experiment results is about 1%. This good agreement provided the good energy dependences of the stage-1 prototypes. For the dosemeter reference direction 0° and for all incident angles in the horizontal plane, the measured response values of the PMMA dosemeter prototype are in the range (R_{min} to R_{max}) 0.87 to 1.02. On the other hand, vertical angular dependences were not really satisfying for the PMMA and PE area dosemeter prototypes.

6.3. Stage-2 prototypes

The main task for developing the stage-2 prototypes was the achievement of better angular dependencies of the *H*(10)* dosemeter responses, especially for incident radiation fields in the vertical plane and near the extreme angles of ±90°*vert*. In addition, some practical aspects should also be improved. The fixation of the dosemeter parts by screwing proofed to be too time consuming for routine applications. Moreover, an aluminium protection case should be introduced similar to the currently used H_x area dosemeter.

Instead of using 3 TLD cards as for the stage-1 prototypes, a 4-card version was tested in this second developing stage, see figure 4 on the left hand side. The additional card was positioned at the centre of the dosemeter. For the inner cylindrical part, the material polycarbonate (PC) was used. Similar to the stage-1 prototypes, the measuring signal is evaluated as the mean value over all TL detector elements of the three symmetrically arranged measuring cards. The signal of the central TLD card could be used for fading corrections, according to the concept of the current H_x area dosemeter.

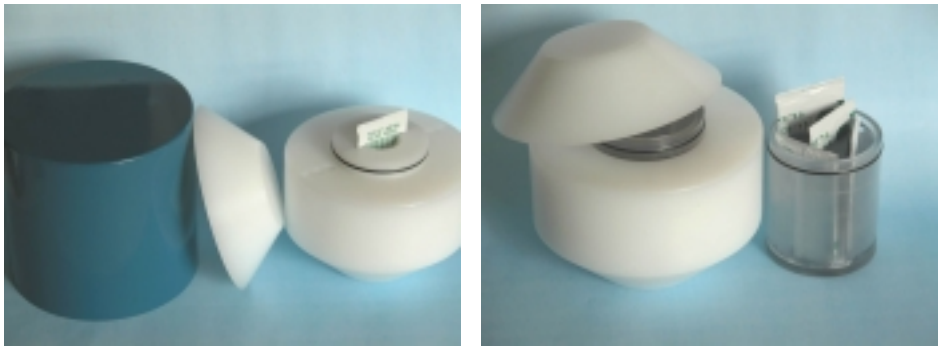

FIG. 4. Photographs of the stage-2 prototype area dosemeters. Left: 4-card PE dosemeter with inner PC part. Right: 1-card PE dosemeter with aluminium case.

Figure 4 on the right hand side shows a stage-2 prototype with only 1 TLD card but with the same shape and dimensions as the 4-card variant. The main reason for developing an additional stage-2 prototype consisting only of 1 central TLD card was the reduced number of TLD cards. Especially for facilities using over hundred area dosemeters the reduced costs could be important. A somewhat increased directional dependence for some angles of incidence and a little increased measuring uncertainty (because of using only 4 instead of 12 TL detector element signals) have to be taken into account for the 1-card prototype employment. The modular construction of the dosemeter similar to the prototypes of stage-1 was also intended for routine applications. For users it would be possible to exchange the inner cylindrical part instead of the whole dosemeter.

6.4. Stage-3 prototypes

The properties of the third-stage area dosemeters of the presented prototyping process are currently under testing. Two variants (1-card and 3-card dosemeter prototypes) were developed, see figure 5 left hand side. They represent the final version of the new *H*(10)* area dosemeter. Only minor adaptations are planned after comprehensive dosimetric measurements and field tests.

The main aims of the stage-3 prototyping were the reduction of size and weight and the simplification of the construction procedures, resulting in lower costs per dosemeter and easier handling. Suitable materials could be employed for dosimetric, mechanical, and environmental conditions showing high temperature, UV light, and chemical resistance.

FIG. 5. Left: Photograph of the inner parts of the stage-3 prototypes.
Right: Field experiment at the borders of the research centre Seibersdorf.

Figure 5 right hand side shows some stage-3 prototypes mounted at the border fence of the radiation protection building of the research centre Seibersdorf. The field tests are carried out simultaneously to the routine measurements with the currently used H_x area dosemeter. Other prototypes are exposed at indoor locations and at low dose level locations. Descriptions and results of the running measurements will be published in the near future.

References

[1] European Council (EC) Directive, Richtlinie des Rates der Europäischen Union zur *Festlegung der grundlegenden Sicherheitsnormen für den Schutz der Gesundheit der Arbeitskräfte und der Bevölkerung gegen die Gefahren durch ionisierende Strahlen,* EC 96/29/EURATOM, Amtsblatt der Europäischen Gemeinschaften Nr. L 159, 1-114, (1996) (in German).

[2] Saez-Vergara, *Recent Developments of Passive and Active Detectors in the Monitoring of External Environmental Radiation,* Radiat. Prot. Dosim. 92(1-3), 83-88, (2000).

[3] Hranitzky, C., *Entwicklung eines auf Thermolumineszenz basierenden Ortsdosimeters zur Bestimmung der Umgebungs-Äquivalentdosis H*(10) in Photonen-Strahlenfeldern,* Master theses, Technical University of Graz, (2002) (in German).

[4] Carlsson, C.A., Alm Carlsson, G., Lund, E., Matscheko, G., Pettersson, H.B.L., *An Instrument for Measuring Ambient Dose Equivalent,* Radiat. Prot. Dosim. 67(1), 33-39, (1996).

[5] Duftschmid, K.E., Hizo, J., Strachotinsky, Ch., *A Secondary Standard Ionisation Chamber for Direct Measurement of Ambient Dose Equivalent H*(10),* Radiat. Prot. Dosim. 40(1), 35-38, (1992).

[6] DIN, *Verfahren zur Umgebungsüberwachung mit integrierenden Festkörperdosimetern*, DIN 25483: 2000-09, Germany, (2002) (in German).

[7] Stadtmann, H., Hranitzky, C., Willer, H., Aigner, B., *Comparison of Exposure and Dose Distribution of different Occupational Groups in Austria*, to be presented at the 11th International Congress of the International Radiation Protection Association, Madrid, (2004).

[8] International Commission on Radiation Units and Measurements (ICRU), *Conversion Coefficients for Use in Radiological Protection against External Radiation,* ICRU Report 57, ICRU Publications, Bethesda, (1998).

[9] American National Standards Institute (ANSI), *Environmental Dosimetry – Performance Criteria for Testing,* ANSI N.13.29 Draft Standard, Pilot testing since (1996).

[10] International Organization for Standardization (ISO), *X and Gamma Reference Radiations for Calibrating Dosemeters and Doserate Meters and for Determining their Response as a Function of Photon Energy –Part3: Calibration of Area and Personal Dosemeters and the Measurement of their Response as a Function of Energy and Angle of Incidence,* ISO 4037-3, Geneva, (1999).

[11] ÖNORM, *Ortsdosimeter zur Messung der Umgebungs- und Richtungs-Äquivalentdosis bzw. –dosisleistung.* ÖNORM S 5237-2 1998-11-01, Österreichisches Normungsinstitut, Vienna, (1998) (in German).

[12] Hranitzky, C., Stadtmann, H., Olko, P., *Determination and Implementation of LiF:Mg,Ti and LiF:Mg,Cu,P Photon TL Efficiencies by Monte Carlo Simulations,* to be presented at the 14th Solid State Dosimetry Conference, NewHaven, (2004).

[13] Briesmeister, J.F., *MCNP –A General Monte Carlo N-Particle Transport Code, Version 4C,* Los Alamos National Laboratory, Technical Report, LA-13709-M, Los Alamos, (2000).

[14] International Organization for Standardization (ISO), *X and Gamma Reference Radiations for Calibrating Dosemeters and Doserate Meters and for Determining their Response as a Function of Photon Energy –Part1: Radiation Characteristics and Production Methods,* ISO 4037-1, Geneva, (1996).

[15] Ankerhold, U., *Catalogue of X-ray Spectra and their Characteristic Data,* PTB-Bericht, PTB-Dos34, ISBN 3-89701-513-7, (2000).

[16] Hraniztky, C., Stadtmann, H., Kindl, P., *The Use of Monte Carlo Simulation Technique for the Design of an H*(10) Dosemeter based on TLD-100,* Radiat. Prot. Dosim. 101(1-4), 279-282, (2002).